



## Evaluation of Uranium Adsorption Using Magnetic-Polyamine Chitosan from Sulfate Leach Liquor of Sela Ore Material, South Eastern Desert, Egypt



CrossMark

Ahmad A. Tolba

Uranium ore processing department, Production sector, Nuclear Materials Authority, El-Maadi, Cairo, Egypt

**C**HITOSAN particles with magnetic properties were prepared by co-precipitation method combined with hydrothermal treatment, then crosslinked with epichlorohydrin followed by grafting of triethylenetetramine. The obtained adsorbent material was characterized by means of FTIR and XRD and its adsorption properties towards uranyl ions were firstly investigated from synthetic solutions as a function of pH, contact time and initial uranium concentration using batch method at room temperature. The maximum adsorption capacity was found to be 158.43 mg/g at pH 4 and initial uranium concentration of 300 mg/l. Urea solution of 0.5 mol/l acidified with a few drops of sulfuric acid 0.2 mol/l can be efficiently used for uranium recovery and the adsorbent can be recycled for at least five successive cycles with limited decrease in adsorption performance. Subsequently, the application efficiency of the adsorbent material was evaluated by testing uranyl adsorption from sulfate leach liquor of Sela ore material after adaptation of leaching conditions. Uranium ore sample was subjected to acid conventional leaching through direct agitation with sulfuric acid and the relevant variables affecting leaching efficiency were optimized as 60 g/l sulfuric acid with liquid/solid weight ratio of 3 at 45°C for 90 minutes. Under these conditions, the leaching efficiency of uranium was 92%. Uranium adsorption capacity from sulfate leach liquor was found to be 132.98 mg/g at pH 4 and shaking time of 60 minutes with initial uranium concentration of 200 mg/l. This adsorption capacity represents only about 87% of the adsorption ability from synthetic solutions (152.86 mg/g) at the same conditions.

**Keywords:** Magnetic-polyamine chitosan, Acid leaching, Uranyl adsorption.

### Introduction

Uranium adsorption using ion exchange resins is a key technology in the uranium mining industry and is well established for the extraction of uranium from both acidic and alkaline leach liquors [1]. Sulfuric acid and sodium carbonate are the most commonly employed leaching agents used to solubilize uranium in acidic and alkaline leach conditions, respectively. The chemistry of these systems causes uranium to form anionic complexes, which can be taken

advantage of by anion exchange resins. These resins have an enhanced ability to preconcentrate aqueous metal species due to the presence of amine functionality which make them readily extract and collect anionic species from aqueous solution [2]. Specifically, anion exchange resins have been the staple choice in both sulphate and carbonate-based uranium processing circuits and are even recognized as the most suitable ion exchangers for uranium recovery, due to their wide pH operating window and acceptable loading capacities [3].

Corresponding author e-mail: [ibn\\_ata@yahoo.com](mailto:ibn_ata@yahoo.com)

Receive Date: 14 April 2020, Revise Date: 24 June 2020, Accept Date: 25 June 2020

DOI: 10.21608/EJCHEM.2020.27972.2586

©2020 National Information and Documentation Center (NIDOC)

However, in the mechanism of any adsorption process there are various kinds of interactions between metal ions and the applied adsorbent can be included such as complexation, ion exchange and physical adsorption [4]. Hence, in the adsorption procedure, the choice of an appropriate adsorbent is a critical factor, whereas the properties of the adsorbent play a key role in the adsorption ability and decides the sensitivity and selectivity of the separation system [5]. In the recent adsorption systems the adsorbents can be optimized with definite properties which make them suitable for specific applications [6].

From this perspective, extensive attention has been focused on developing new adsorbents with high selectivity, cost-effectiveness and high capacity [7]. Therefore, uranium adsorption from different aqueous solutions has been extensively investigated with a great variety of adsorption materials used including inorganic oxides [8, 9], zeolites [10, 11], silica [12, 13], clays [14, 15], carbon-based sorbents [16, 17], composite and hybrid materials [18, 19], bio-adsorbents and natural polymers [20-23]. However, the use of natural polymer based adsorbents appears to be one of the most promising of these alternative adsorption materials.

It is accepted that, certain natural polymers derived from biomass can function similarly to synthetic polymers such as ion-exchange and chelating resins in recovering valuable metal ions and in removing toxic metal ions. Such polymers appear to be potentially useful as adsorbent materials for collecting various metal ions in industrial and analytical applications, because of their low production costs and their excellent collection ability for multivalent metal ions [24]. Moreover, other properties of natural polymers, including renewability, biodegradability, wide availability, non toxicity, etc., make them a favorable choice as sustainable alternatives to the synthetic polymer based materials [25]. Therefore, recently there are many studies have been focused on the development of alternative adsorbents produced from low-cost resources to the traditional synthetic adsorbents, and more specifically materials of biological origin which can be used for the removal of different metal ions, whereas, some of these materials exhibit quite high adsorption capacities [26]. Natural polysaccharides such as chitin, chitosan, and cellulose, and their

derivatives have a wide range of industrial and medical applications because of their unique structure and distinctive properties [27].

Chitosan is the N-deacetylation product of chitin, a biopolymer that can be formulated into beads and films, and the second most abundant naturally occurring biopolymer next to cellulose. Chitosan has received considerable interest for heavy metals removal due to its excellent metal-binding capacities and low cost as compared to activated carbon which considers the most popular and widely used adsorbent in wastewater treatment applications throughout the world [28]. Also, chitosan has attracted the attention due to its intrinsic adsorption properties in addition to the presence of large number of hydroxyl groups, and active primary amino groups with the ability to adopt the suitable configuration for complexation with metal ions due to the flexible structure of the polymer chain [29]. The adsorption performance and selectivity of chitosan based adsorbents can be improved through a relatively simple chemical modification techniques based on grafting various functional groups to chitosan backbone due to the existence of reactive hydroxyl and amino groups [30]. Also there are several modifications have been proposed in order to improve pore size, mechanical strength and chemical stability of these adsorbents [31].

In this study, magnetic chitosan particles were prepared by chemical co-precipitation of ferrous and ferric ions using sodium hydroxide in the presence of chitosan dissolved in acetic acid solution and then followed by hydrothermal treatment. Polyaminated adsorbent has been developed through post chemical modification of the previously prepared magnetic chitosan particles with triethylenetetramine after using epichlorohydrin as crosslinking agent. The obtained material was characterized by means of FTIR spectrometry and XRD analysis and its adsorption properties toward uranyl ions from synthetic solution were investigated at room temperature using batch experiments as a function of pH, contact time, initial metal ion concentration. Also, uranium recovery from adsorbent phase, as well as, adsorbent recycling was investigated. At the end of the work, the application efficiency of the prepared material as effective adsorbent was tested and evaluated through the adsorption of uranyl ions from

optimized sulfuric leach liquor of Sela ore material after adaptation of leaching conditions.

## Experimental

### Reagents and analysis

Chitosan (90.5% deacetylation degree) and Triethylenetetramine ( $\geq 97\%$ ) were purchased from Sigma-Aldrich. Epichlorohydrin ( $>98\%$ ), Arsenazo III and ethanol were obtained from Fluka Chemicals, while all other chemicals were Prolabo products and used as received. Uranium stock solution was prepared from  $\text{UO}_2(\text{OCOCH}_3)_2 \cdot 2\text{H}_2\text{O}$ , supplied by Sigma-Aldrich, by dissolving appropriate quantity in lowest amount of concentrated sulfuric acid under heating and finally diluted with double distilled water to final concentration of 1000 mg/l. The solutions were prepared by appropriate dilution of the stock solutions immediately prior to use. Uranium concentrations were determined by spectrophotometry using Arsenazo III colorimetric method [32] and by using UV-Visible spectrophotometer (Metertech Inc, model SP-8001). The pH of the uranium solutions was adjusted using either 0.2 mol/l NaOH or 0.2 mol/l  $\text{H}_2\text{SO}_4$  solutions.

### Synthesis of the adsorbent

Chitosan (3 gm) was dissolved in 150 ml (20% w/w) acetic acid solution before adding  $\text{FeSO}_4$  and  $\text{FeCl}_3$  salts with a molar ratio of 1:2 Fe(II)/Fe(III) and the resulting solution was chemically precipitated at  $40^\circ\text{C}$  by dropwise addition of 2 mol/l NaOH under constant stirring, the pH being controlled to 10. The suspension was heated at  $90^\circ\text{C}$  for 1 h under continuous stirring before being separated by decantation [33]. After that, an alkaline solution 0.01 mol/l epichlorohydrin (in 0.067 mol/l NaOH) was prepared with pH about 10 and added to a freshly prepared suspension of wet magnetic chitosan particles (the mass ratio was 1:1) and the mixture was heated for 2 h under constant stirring at  $40\text{--}50^\circ\text{C}$  [34]. The obtained material was finally filtered off and extensively washed with double distilled water to remove any unreacted epichlorohydrin.

The triethylenetetramine functionality was grafted on the cross-linked magnetic particles of chitosan in two steps. Firstly, the cross-linked magnetic particles were suspended in 115 ml of

ethanol/water mixture (1:1 v/v) and epichlorohydrin (11.5 ml) was added to the suspension under agitation and reflux for 4 h [35]. Then, the product was filtered off and washed three times successively with ethanol and double distilled water to remove any residual reagent. Secondly, the product was suspended in 150 ml ethanol/water mixture (1:1 v/v) and 13.75 ml of triethylenetetramine were added. The mixture was stirred at  $75\text{--}80^\circ\text{C}$  for 18 h [36]. After the reaction, the final product was filtered off and extensively washed with ethanol and double distilled water. Finally, the adsorbent was dried at room temperature for at least 24 h.

### Adsorbent characterization

The chemical composition of the prepared adsorbent was characterized by means of Fourier transform IR spectrometer Nexeus-Nicolite Model 640-MSA and Philips X-ray generator model PW 3710/31 a diffractometer with automatic sample changer model PW1775, in order to obtain FTIR spectra and XRD patterns, respectively. Moreover, amine content in the adsorbent phase was estimated using a volumetric method [36], 30 ml of 0.05 mol/l HCl solution was added to 0.1 gm of the dry adsorbent and equilibrated under agitation for 15 h on a mechanical shaker. The residual concentration of HCl was estimated by back titration against 0.05 mol/l NaOH solution and phenolphthalein as indicator. The number of moles of HCl has been reacted with amino group and consequently the amino group concentration in mmol/g was calculated by the following equation:

$$\text{Amino group Conc., mmol/g} = (M_1 - M_2) V / wt$$

Where  $M_1$  and  $M_2$  are the initial and final concentrations of HCl in mol/l respectively,  $V$  is the volume of HCl acid solution in ml and  $wt$  is the weight of the dry adsorbent in gram.

### Adsorption and desorption experiments

Batch experiments were carried out by placing portions of 100 mg magnetic-polyamine chitosan adsorbent in contact with 100 ml of aqueous sulfate solution with metal ion concentration of 150 mg/l in a series of stopper conical flask. Then, the flasks were equilibrated by shaken on a mechanical shaker of Denley type with A500 orbital mixer at 250 rpm for

three hours at room temperature. After equilibration and phase separation, the residual uranium concentration in the aqueous phase was determined as previously mentioned, and consequently the concentration of the adsorbed metal ions onto the adsorbent phase (adsorption capacity, in mg/g) can be obtained by the following equation:

$$\text{Adsorption capacity, } q_e \text{ (mg/g)} = (C_i - C_f) V / wt$$

Where  $C_i$  and  $C_f$  are the initial and final uranium concentrations in the aqueous solution (mg/l),  $V$  is the volume of aqueous solution (L) and  $wt$  is the weight of dry adsorbent (g).

However, these parameters were varied during the optimization of the adsorption process in order to determine the effect of contact time, initial metal ion concentration, as well as, adsorbent recycling and reusability. The adsorbent recycling was tested by comparing the adsorption capacity for different successive sorption/desorption cycles by mixing and shaking of 100 mg adsorbent with 100 ml of a uranyl solution with metal ion concentration of 200 mg/l for 60 minutes at room temperature in a conical flask. After phase separation the adsorbent was recovered and the uranium concentration in the aqueous solution was determined. After that, the previously metal-loaded adsorbent, after washing with double distilled water, was mixed with 50 ml of a 0.5 mol/l urea solution acidified with a few drops of 0.2 mol/l  $H_2SO_4$  for 30 min at room temperature. The metal concentration in the eluted solution was used for calculating the desorption efficiency at each step of recycling. Elution efficiency was calculated from the amount of metal ion adsorbed on the adsorbent phase at equilibrium and the final metal ion amount in the eluate volume according to the following equation:

$$\text{Desorption efficiency, \%} = (C_{de} \times V / q_e \times wt) 100$$

Where  $C_{de}$  (mg/l) is the metal ion concentration in the eluate solution after desorption,  $V$  (L) is the volume of the eluate solution,  $q_e$  (mg/g) is the adsorption capacity for metal-loaded adsorbent at equilibrium, and  $wt$  (g) is the amount of the metal-loaded adsorbent used in the desorption experiment.

#### *Uranium leaching from Sela ore material*

A technological representative sample of Sela uranium ore material from southern eastern desert of

Egypt (Latitudes: 22°14'30"-22°18'36" N / Longitudes: 36°11'45"-36°16'30" E) with uranium assay of 1034 ppm was obtained from an ore deposit of G. El Sela area, at a distance of about 60 km south west of Abu Ramad City. The ore material sample was first crushed and grinded to the liberation size appropriate for uranium dissolution and until the whole sample passed through 150  $\mu$ m sieve. Then the sample was thoroughly mixed and dried at 110 °C. After that, the sample was subjected to complete chemical analysis to determine its major oxides. The obtained results are given in Table 1. From which we could observe the presence of high content of  $Al_2O_3$  (14.63 %),  $Fe_2O_3$  (6.13 %) and L.O.I (6.15 %) which may be seems to reflect the intensive alteration of clay materials.

The uranium ore sample of Sela was subjected to acid conventional leaching through direct agitation with sulfuric acid. Relevant variables affecting uranium leaching efficiency such as acid concentration, liquid/solid weight ratio, leaching time and temperature were studied in order to determine the optimum leaching conditions. The effect of oxidant has not been studied since uranium is almost exclusively present in its hexavalent state. The leaching experiments were performed in proper glassware containers and the reaction medium was heated using a hot plate with magnetic stirrer and a thermostat is employed to keep the reaction medium at constant temperature. In the leaching process, sulfuric acid solution with known volume and concentration was mixed with specific amount of the ore sample and the desired temperature was adjusted under stirring at 350 rpm for a certain period of time. After that, the solution was filtered off where the reacted slurry was subjected to filtration through buchner funnels using a laboratory vacuum pump. Furthermore, due to occurrence of turbidity, another filtration step was required to clarify the pregnant leach liquor. Uranium concentrations in the leaching filtrate were determined by titration to avoid the interference in spectrophotometry method where uranium analysis was performed using the oxidimetric titration method [37]. Uranium leaching efficiency was calculated by referring the leached metal amount in the leach liquor to its original input value according to the following equation:

*Leaching efficiency, % = (Dissolved U, mg / the input amount of U in the sample, mg) 100*

## Results & discussion

### *Adsorbent synthesis*

Generally, in order to prepare magnetic chitosan particles, the two-step procedure was frequently employed. This procedure consists of synthesizing  $\text{Fe}_3\text{O}_4$  particles followed by binding them with chitosan particles. Practically, there are two binding methods can be applied. The first one is verse-phase suspension cross-linking method and the second one is precipitation method [38]. In both methods the size of the particles was mostly in micrometer scale. However, in comparing with the verse-phase suspension cross-linking method, the precipitation method is quite simple and facile to be carried out, especially in post-treatment [33]. Therefore, magnetic chitosan particles were prepared using precipitation method combined with hydrothermal treatment, through one-step process involving the co-precipitation of ferrous and ferric ions simultaneously with chitosan particles. Under selected experimental conditions, magnetite particles were spontaneously produced whereas the pH change caused precipitation, simultaneous co-precipitation and embedding of magnetic particles with chitosan particles. Moreover, the dropwise addition of sodium hydroxide solution to the suspension mixture under constant stirring leads to the formation and stabilization of micrometer-sized magnetic chitosan particles [39].

Also, in order to make the adsorbent material insoluble in highly acidic aqueous solution and to stabilize chitosan in a wider pH range, the polymer chains of magnetic chitosan would be cross-linked to enhance its mechanical strength and chemical resistance. As known, chitosan have a large number of active primary amino and hydroxyl groups. Therefore, the polymer chains can be cross-linked through the reactions on primary amino groups using glutaraldehyde either or through the reactions on primary hydroxyl groups using epichlorohydrin. Herein, epichlorohydrin was preferred than aldehyde for magnetic chitosan cross-linking in order to prevent the loss of amine groups reactivity which will be utilized in the next step of adsorbent modification. Subsequently, in order to produce a spacer arm

within the adsorbent matrix for bearing polyamine functionality, the previously cross-linked magnetic chitosan particles, were reacted again with epichlorohydrin in water/ethanol solution. Under selected experimental conditions, the crosslinking agent (epichlorohydrin) this time was reacted with the amino groups and leaving its chloride terminal ends for further reaction of grafting triethylenetetramine. The proposed route for chitosan crosslinking using epichlorohydrin and triethylenetetramine grafting was schematically illustrated in Figure 1.

### *Adsorbent characterization*

#### *FTIR analysis*

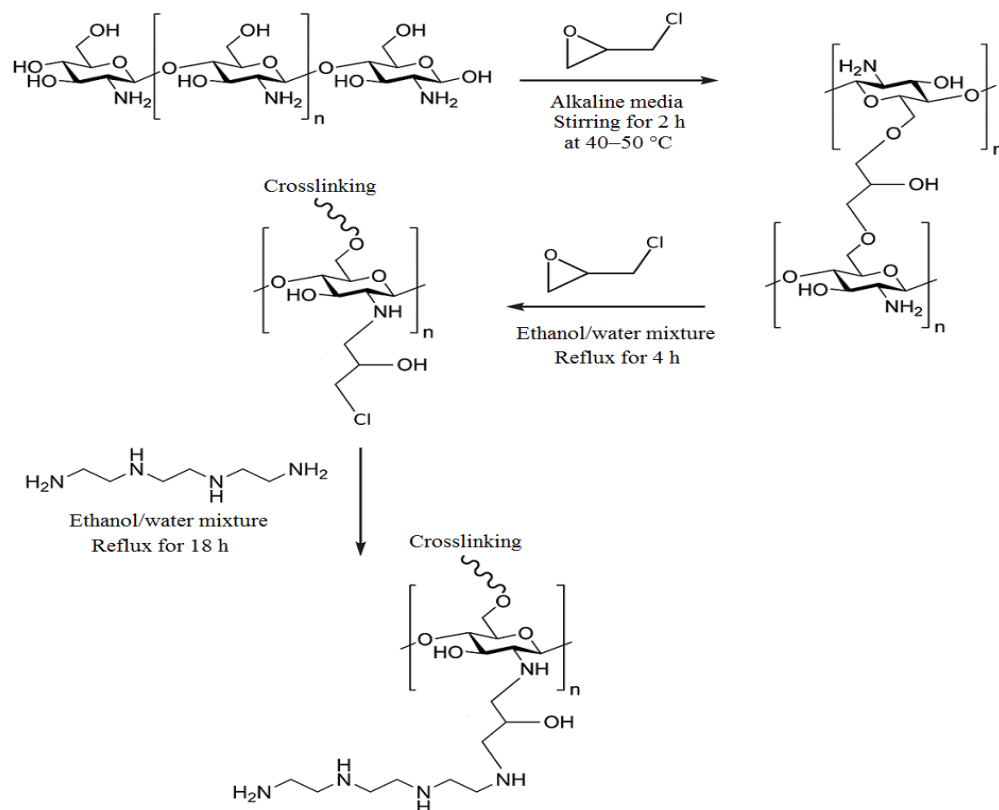
FT-IR spectroscopy has been utilized to identify the functional groups which represent the active sites on the adsorbent and also to confirm the successive chemical modifications of the biopolymer matrix. The FTIR spectra of raw chitosan, magnetic chitosan and magnetic-polyamine chitosan particles have been reported in Figure 2. Basically, the three spectra were similar and the main differences were identified in terms of relative intensity. The spectrum of raw chitosan was characterized by large and broad band at  $3372\text{ cm}^{-1}$  corresponding to the combination of contributions from stretching vibration of O-H groups, extension vibration of N-H groups and the inter-hydrogen bonds of polysaccharides. The band at  $2879\text{ cm}^{-1}$  is associated to stretching vibration of C-H groups. The bending vibrations of mine group -NH<sub>2</sub> are appearing at  $1596\text{ cm}^{-1}$ , while the stretching vibrations of primary -OH and secondary -OH groups are identified at  $1314$  and  $1021\text{ cm}^{-1}$ , respectively. The bands at  $1459$  and  $1388\text{ cm}^{-1}$  can be assigned to C-O-C stretching and -OH bending vibrations, respectively. The  $\beta$ -D-glucose unit is identified by the band at  $881\text{ cm}^{-1}$ . On the other hand, the presence of iron magnetite embedded within chitosan particles can be confirmed by the appearance of the band at  $589\text{ cm}^{-1}$ , which is assigned to the Fe-O stretching vibration of  $\text{Fe}_3\text{O}_4$  [33]. The cross-linking of chitosan, as well as, spacer arm production by using epichlorohydrin will cause a decrease in the absorption intensity of -NH<sub>2</sub> and -OH groups compared to raw chitosan material, which is explained by the substitution of hydrogen atoms when chitosan was crosslinked through primary hydroxyl groups followed by the insertion of spacer

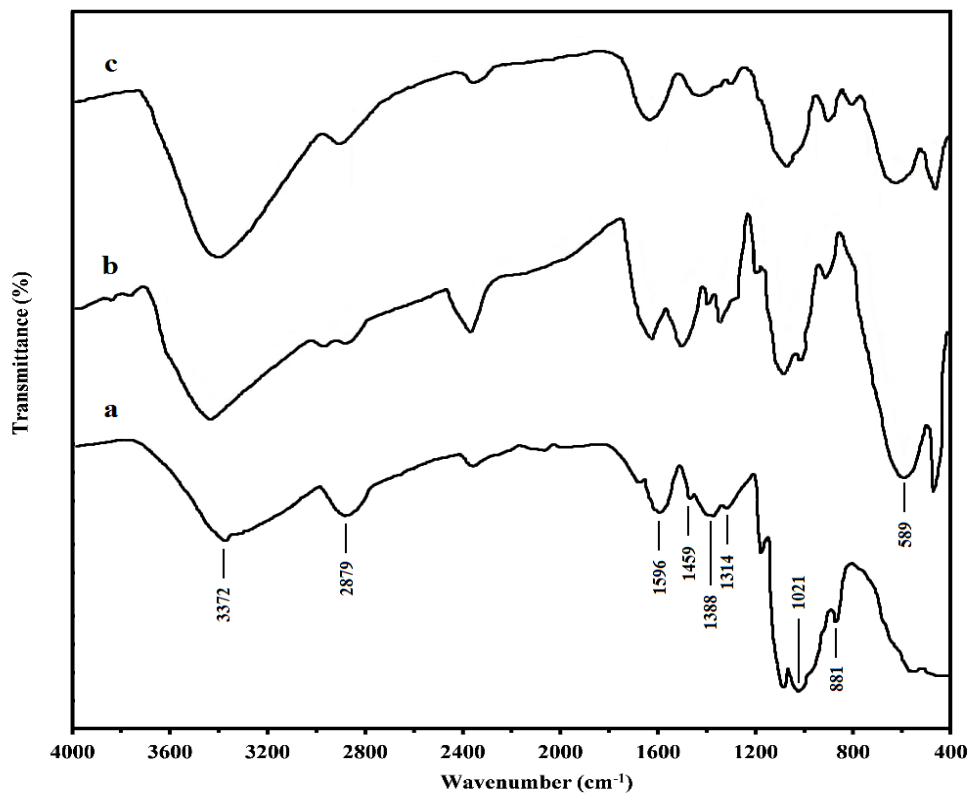
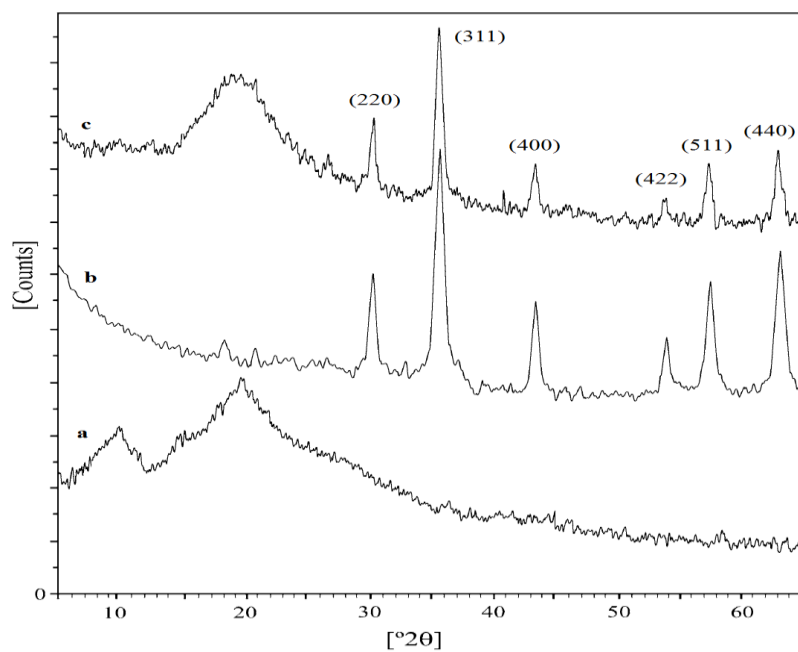
arm on amino groups. However, the grafting of amine functionality was accompanied with an increase in the intensity of primary and secondary amine groups which will compensate the former decrease in the absorption intensity of amine groups. Therefore, there is no a clear difference between the three spectra in this concern and they are very similar except for the variation in the intensity of the bands relative to amine groups. These bands can be correlated to the results of amine content which was volumetrically determined before and after grafting of triethylenetetramine and were found to be 2.13 and 4.28 mmol/g, respectively. These results mean that, the amine content become about two times greater than that before grafting which reflects a successful chemical modification consistent with the proposed structure of functionalized chitosan.

#### XRD analysis

The X-ray diffraction patterns have been compared for raw and magnetic chitosan particles in reference to pure magnetite particles, the recorded patterns have been reported in Figure 3. In general, chitosan material is poorly crystalline and characterized with a relatively large peak located

close to  $2\theta = 20^\circ$  and another smaller peak located close to  $2\theta = 10^\circ$ , that can be attributed to chitosan chain alignment controlled by intermolecular interactions. After chemical modification, the weak crystallinity of the biopolymer is drastically reduced and the polymer is turning to amorphous structure. The large peak was broadened and shifted toward higher  $2\theta$  with disappearing of the smaller peak. The intercalation of reactive groups in the polymer network and the disruption of hydrogen bonds between the chains can explain this decrease of the crystallinity which makes the structure less organized. From the XRD patterns, six characteristic peaks for magnetite ( $2\theta = 30.1, 35.4, 43.0, 53.5, 57.0$  and  $62.5$ ) marked by their indices [(220), (311), (400), (422), (511), and (440)] were observed for both samples of pure magnetite and magnetic chitosan particles. These peaks are consistent with the database in JCPDS file (PDF No. 65-3107) and reveal that the resultant magnetic particles were iron oxide particles ( $\text{Fe}_3\text{O}_4$ ) with a spinel structure [6, 39]. These obtained results reflect the incorporation of a magnetic core in the adsorbent particle and the presence of iron oxide within the polymeric matrix.



**Fig. 1. Scheme for chitosan crosslinking and triethylenetetramine grafting.****Fig. 2. FTIR spectra of raw chitosan (a), magnetic chitosan (b) and magnetic-polyamine chitosan(c).****Fig. 3. XRD patterns of raw chitosan (a), pure magnetite particles (b) and magnetic chitosan(c).**

### *Adsorption properties and performance*

Uranium solution chemistry has a strong dependence on pH, ionic strength, solution composition with respect to the presence of other ions and the redox potential of the system [40]. Due to its relatively complex chemistry, there is no one material that is universally selective for uranium over other metal ions. Designing a uranium-selective separation system requires a careful consideration of the behavior of both reactive groups present in adsorbent phase and uranium species present in aqueous phase at a given set of conditions.

### *pH effect*

The pH value of the aqueous solution is a critical parameter which plays an important role in the whole adsorption process performance and particularly on the adsorption capacity. It can make influences on the surface charge of the adsorbent and its degree of ionization. Whereas, protonation and deprotonation of amino groups at the surface of the adsorbent changes the overall charge of the material and its capacity to bind charges species due to electrostatic attraction or repulsion. Therefore, pH is one of the most important parameters, especially for ionic type adsorbents which having acid-base properties such as ion exchange characteristics [16]. On the other hand, the pH has a great impact on metal speciation; this may include controlling the formation of extractable species in addition to unextractable and/or insoluble species. In the aqueous chemistry of uranium, both metal concentration and pH influence the speciation of the metal through the formation of many different uranyl species including hydrolyzed species, polynuclear species and insoluble uranyl hydroxide. These different uranyl species may be neutral, cationic or anionic with different affinities for the reactive groups present on the adsorbent.

In order to determine the equilibrium pH, The effect of initial pH on the adsorption performance of uranyl ions was investigated in the range from 1 to 7, adjusted by using either 0.2 mol/l  $\text{H}_2\text{SO}_4$  or 0.2 mol/l NaOH, while other variables were fixed at 100 mg of chitosan adsorbent, 100 ml aqueous sulfate solution with initial uranium concentration of 150 mg/l and shaking time of 3h at 250 rpm and room temperature. The obtained results are shown in Figure 4a, from which we can see that, uranyl ions could be adsorbed

quite efficiently in the pH range 4 – 5 and reached adsorption capacity of 127.68 mg/g at equilibrium pH 4. This can be explained by the formation of an ion-pair between uranyl sulfate anions with the positively charged ammonium ions and/or may be attributed to complex formation between the nitrogen lone pair of electrons and metal ion. While, with the further increase in the pH from 5 to 7, uranyl ions adsorption slightly increased, probably due to the formation of different uranyl species with different adsorption affinities such as uranyl hydroxides, including polynuclear and polyhydrolyzed species in addition to colloidal species that can precipitate in the solution or at the surface of the adsorbent [41]. Also, the weak variation of adsorption capacity above pH 5 may be due to the buffering-like effect of the adsorbent caused by its acid-base properties. The lower adsorption capacity values observed in the pH range from 1 to 3 may be attributed to the increased extent of protonation of amino groups as the pH decreases with the predomination of neutral uranyl sulfate species with the presence of uranyl oxy-cation with lower adsorption affinities and a lower fraction of the extractable anionic uranyl sulfate species. While, the adsorption capacity was increased from 75.46 to 127.68 mg/g when the pH was increased from 3 to 4 and remain constant till pH 5, which may be due to the formation of different anionic uranyl sulfate species with higher adsorption affinities. Thus, for further experiments the pH of solutions was systematically fixed to 4 allowing maximum adsorption capacity and preventing the pH variation to cause the possible uranyl precipitation at high metal ion concentration.

It is clear that, the adsorption performance and binding mechanism of uranyl ions is pH dependent with different types of mechanisms may be involved including ion exchange, chelation, adduct formation and molecular addition mechanisms. Whereas, the effects of hydrogen ion concentration on the adsorption of uranyl ions from sulfate media is much more important than that in the case of chloride and nitrate media. This can be understood in the view of the effect of pH variation on the sulfate-bisulfate equilibrium and the ability of bisulphate anion to compete with metal sulfate anion for adsorption. In strong acidic solutions with lower pH values, reactive amino groups which present in the adsorbent phase

are protonated, which results in positively-charged surface with the presence of bisulphate anion as the major anionic species, which in turn would hinder uranium adsorption. This behavior can be explained on the basis of stepwise dissociation of sulfuric acid to give a bisulfate anion and a proton in the first step and sulfate anion and the other proton in the second step depending on the hydrogen ion concentration of the aqueous solution. Herein, at these conditions uranyl binding occurs by ion exchange of the lower fraction of anionic uranyl sulfate species on protonated amine groups, and the adsorbent become poorly efficient for binding neutral uranyl sulfate species and free cationic uranyl due to the impact of electrostatic repulsion. While, as the acid concentration is decreased and pH was increased the sulphate ions predominant and the protonated amine groups would gradually deprotonate which in turn reduce the repulsion effect of the adsorbent surface for metal cationic species and significantly enhances the electrostatic interaction between the adsorbent and charged metal ions, which in turn will lead to an increase the adsorption capacity as a consequence. Also, the deprotonation of amine groups makes the nitrogen free lone pair of electrons available for complexation and coordination with metal ions. Therefore, by increasing pH above 5 and until near neutral pH, the free uranyl cations as well as uranyl polynuclear and/or poly-hydrolyzed species can be strongly bounded to free amino groups by chelation mechanism.

#### *Contact time effect*

Chitosan based adsorbents can be considered more hydrophilic than many other conventional synthetic materials such as polystyrene-divinylbenzene, polyethylene and polyurethane. This hydrophilic behavior associated with the presence of numerous hydroxyl groups, which is expected to enhance adsorption kinetics in aqueous solutions [42]. Moreover, the adsorption kinetics is usually controlled by the intrinsic reaction rate and by steps of resistance to bulk diffusion, film diffusion and intra-particle diffusion. However, with providing a sufficient agitation to the adsorption system would allow to minimize the limiting effects of bulk and film diffusions. In order to determine the required time for equilibrium, the effect of contact time on the adsorption performance of uranyl ions was

investigated in the range from 15 to 180 minutes, while other variables were fixed at 100 mg of chitosan adsorbent and 100 ml aqueous sulfate solution with pH 4 and initial uranium concentration of 150 mg/l were shaken at 250 rpm and room temperature. The obtained results are shown in Figure 4b, from which we can observe that, the adsorption rate of uranyl ions was proceeding rapidly, where within the first 30 minutes the adsorption capacity reached 85.21 mg/g which represent 69.63 % from the total uptake capacity at the end of the whole adsorption time of 180 minutes. The adsorption rate exhibits a regular increasing till 60 minutes with a slight increase in the adsorption after one hour. Moreover, adsorption time of 60 minutes represents the inversion point of the adsorption curve and it was found to be enough to achieve adsorption capacity of 122.36 mg/g which corresponding to 94.5 % from the total uptake capacity at the end of the studied adsorption time. It is worthy to mention that, the increase in adsorption capacity by increasing contact time from 60 to 90 minutes doesn't exceed 7 mg/g, while after 90 minutes there is no considerable effect. Accordingly, contact time of 60 minutes was depended as equilibrium time.

Also, it is clear that, uranyl ions adsorption mainly consists of two stages, an initial rapid stage related to the instantaneous external surface adsorption of metal ions with the more available reactive groups. Where, fast adsorption equilibrium was reached in the first 45 minutes with adsorption capacity of 101.13 mg/g which was about 80% from the total adsorbed uranyl ions at the end of the whole adsorption time. This could be due to the high specific surface area of the adsorbent particles and absence of internal diffusion resistance in this stage [38]. As these sites became progressively covered, the rate of adsorption decreased. The second stage is much slower with gradual adsorption levels take place and lasts till metal ions adsorption attains equilibrium, which attributed to the diffusion of metal ions into the polymer layers for binding on the inner reactive groups, with the aid of hydrophilic and swelling characters of the adsorbent material. Moreover, the formation of uranyl poly-nuclear and poly-hydrolyzed species, which are characterized by larger ion size, may be contribute to the slowdown of the mass transfer in the second phase of adsorption

process. Since their diffusion in the porous network of the polymer may be hindered by this increased ionic size. Also, the formation of polynuclear species and their adsorption at the external surface may be the responsible for the faster decrease in uranium concentration, where every polynuclear molecule bound represents 2 to 4 bound uranyl entities. Therefore, the initial adsorption uptake rate is increased while the second step is slowed down with formation of polynuclear species.

#### *Initial uranium concentration effect*

The embedded magnetite particles within the adsorbent phase are expected to contribute in the improvement of adsorption properties and particularly on the adsorption capacity. This may be due to the formation of extended polymeric film of the adsorbent over magnetite particles. This thin film formation would result in a higher exposed active sites as well as good chance for interaction with metal ions [43]. In order to determine the maximum adsorption capacity which is considered of prime importance for applicability considerations, the effect of initial uranium concentration on the adsorption performance of uranyl ions was investigated in the range from 50 to 400 mg/l, while other variables were fixed at 100 mg of chitosan adsorbent and 100 ml aqueous sulfate solution with pH 4 and shaking time of 60 minutes at 250 rpm and room temperature. The obtained results are shown in Figure 4c. The adsorption curve indicates that, the uptake of uranyl ions increases as the initial concentration of the metal ion increased until it reaches maximum adsorption capacity at the plateau region; then the further increase has no effect on the adsorption capacity. The adsorption capacity of the applied adsorbent is the maximum amount of adsorbed metal ions that the adsorbent phase can hold at equilibrium and it was found to be 158.43 mg/g at an initial uranium concentration of 300 mg/l. Thereafter, the adsorbed amount of uranium remained constant, expressing that the adsorbent was reached to its maximum adsorption capacity. From the obtained results, an initial uranium concentration of 200 mg/l was found to be enough to achieve 152.86 mg/g, which corresponds to 96.48 % of the total adsorption capacity at an initial concentration of 300 mg/l. It is worthy to mention that, the increase in the adsorption capacity of uranium by increasing the initial concentration

from 200 to 250 mg/L during the adsorption doesn't exceed 4 mg/g. Therefore, an initial uranium concentration of 200 mg/L was chosen to be the equilibrium concentration.

The distribution of uranyl ions between liquid phase and solid phase at equilibrium depends on the solution pH and the metal ions concentrations. The adsorption isotherm represents this distribution curve for different metal concentrations at fixed pH value and constant temperature. Figure 4d represents the adsorption isotherm curve of uranyl ions, which describes the relationship between adsorption capacities in the solid phase against the remaining uranium concentrations in the aqueous phase at equilibrium. The isotherm is regular, positive, and concave to the concentration axis. The initial rapid adsorption gives way to a slow approach from saturation at higher metal ion concentrations. Also, it is clear that, these adsorption results reflect the efficiency of the adsorbent for the recovery of uranium ions from sulfuric acid solutions in a wide range of concentrations, especially from diluted solutions with low concentrations, where the percent of uranyl ions recovery from solution with an initial metal ion concentration of 50 mg/l exceeded 97% with an adsorption capacity of 48.78 mg/g and for a solution with an initial metal ion concentration of 100 mg/l the recovery percent reached about 94% with an adsorption capacity of 93.84 mg/g. This indicates that, at lower initial metal ion concentrations, the adsorption sites on the adsorbent surface were sufficient for the metal ions recovery, where the adsorption relied on the amount of metal ions transported from the bulk aqueous solution to the surface of the adsorbent only. While, at higher initial concentrations of uranyl ions, the adsorption sites on the surfaces of the adsorbent as well as that present in the bulk phase would reach to saturation, before the adsorption of uranyl ions achieved equilibrium.

In the adsorption systems, the adsorption behavior is due to the formation of a definite stable metal species and the saturation capacity is restricted by the molar ratio of the active sites present in the adsorbent phase to metal ions in these species. Thus, the usefulness of polyamine chitosan particles as adsorbent is usually considered to depend essentially on the ability of uranyl ions to form adsorbable species in the aqueous phase in addition to the

concentration of amino group in the adsorbent phase. Herein, the co-existence of different uranyl species and the possibility to adsorb different species make a difficult discussion about stoichiometric ratios as it is difficult to support a definite adsorption mechanism based only on uranyl ions and amino group molar ratios. Where, the involved adsorption mechanism and adsorption affinity are strongly changed with the polarizability of the reactive groups during the proceeding of the adsorption process. Also, depending on the impact of hydrogen ion concentration on ionic affinities of the amino groups due to the acid-base properties of the adsorbent, in addition to, the chemical and steric environment of reactive groups which are significantly different.

Under definite adsorption conditions, ion-exchange mechanism between anionic uranyl sulfate species and the ion-pair of the protonated amino groups can be present with a poor affinity for cationic and/or neutral uranyl species that can be demonstrated during these conditions. While, under other conditions metal ions favors the formation of potentially more adsorbable species  $\text{UO}_2(\text{SO}_4)_2^{2-}$  and  $\text{UO}_2(\text{SO}_4)_3^{4-}$  and the involved mechanism turns to coordination where these species can be bound to deprotonated amine groups by chelation, as well as, adsorption with ion-exchange mechanism. These behaviors may be explaining the significant differences in uranyl adsorption mechanisms that may be involved.

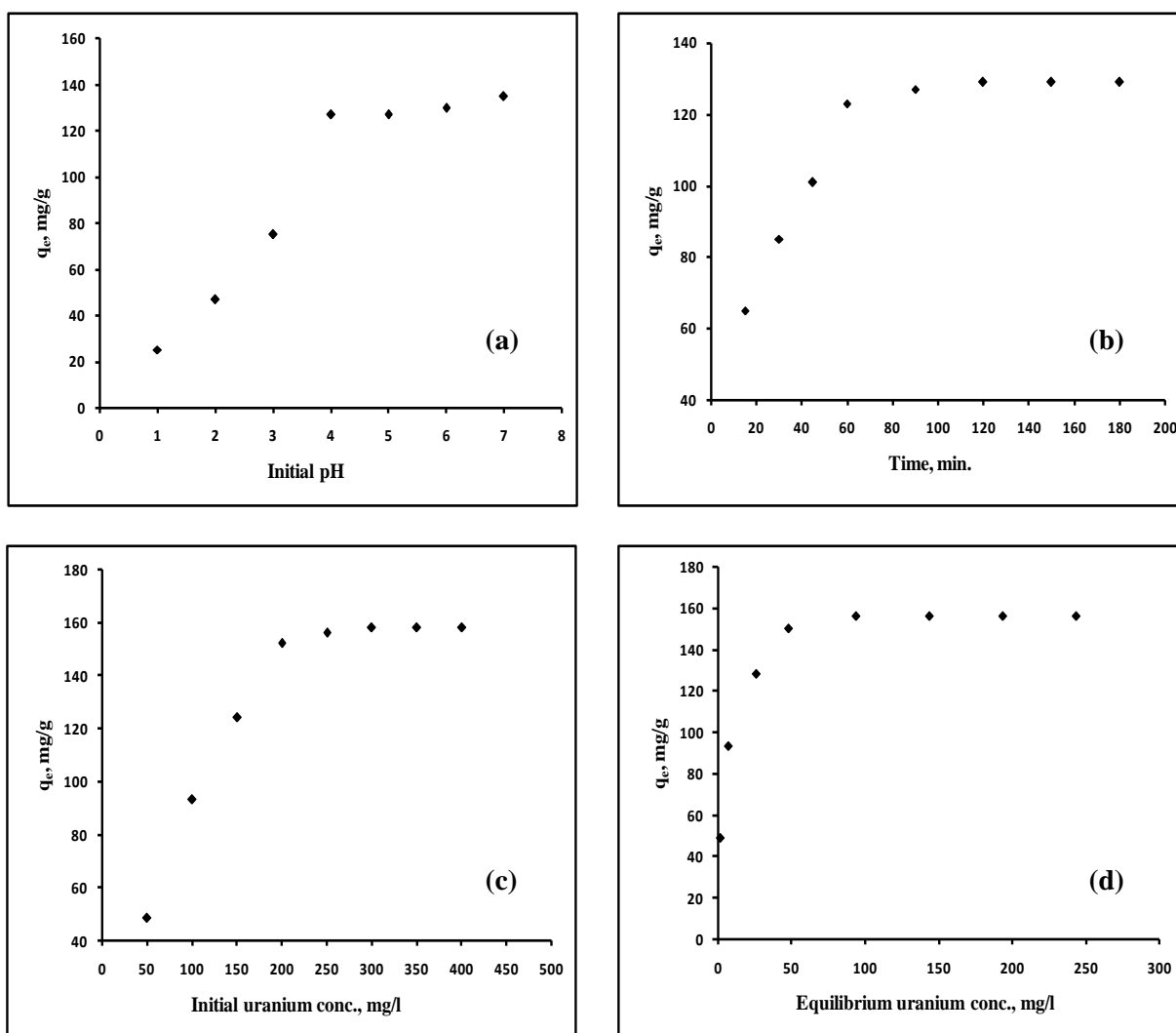
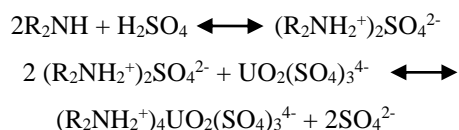


Fig. 4. Effect of different variables on uranyl ions adsorption.

Theoretically, by assuming ion exchange mechanism between the more adsorbable anionic uranyl sulfate species  $\text{UO}_2(\text{SO}_4)_3^{4-}$  and the ion-pair of the protonated amino groups, the molar ratio of amine groups to uranyl ions would be 4 to 1 where four moles of amine would be consumed for adsorption of 1 mole of uranyl sulfate [44]. Firstly, the amine should be converted to the appropriate amine salt or polar ion pair in a manner that provides an anion to be exchanged with the metal species through extraction of an acid as illustrated in the following equations:



Based on the above equation, the expected amount of uranyl ions to be adsorbed by 1 g of chitosan adsorbent containing amine concentration of 4.28 mmol/g (which was volumetrically determined after grafting of triethylenetetramine functionality) is about 1.07 mmol of uranyl ions for one gram of chitosan adsorbent, which corresponding to 254.66 mg uranium per gram of adsorbent. The experimental result which was found to be 158.43 mg/g represents only 62.21 % from the expected value for the adsorption capacity. This behavior can be explained if we consider that, the amine active sites present in the adsorbent phase may be divided into active outer layer and shielded inner layer which may become inactive by blocking with the adsorbed amine-metal complex with larger ionic size. Hence, not all amine content available for uranyl ions adsorption and consequently the practical adsorption capacity of the adsorbent was strongly less than that calculated theoretically.

#### *Uranium desorption and adsorbent recycling*

Many desorption procedures for several metal ions from various types of loaded adsorbents were commonly performed using acidic solutions. But here, high acidic conditions may be cause a partial dissolving and destruction of the magnetic core of adsorbent particles. Therefore, alternative eluants such as carbonate and bicarbonate solutions, ethylenediamine tetraacetic acid, thiourea and urea, which are known for being strong chelating agents

for numerous metal ions, were tested to replace the active groups of the adsorbent and preferentially complex with metal ions. Preliminary performed tests showed that, 0.5 mol/l urea solution acidified with few drops of 0.2 mol/l sulfuric acid was effectively desorbs uranyl ions and contact time of 30 minutes was sufficient for achieving desorption equilibrium. The adsorbent recycling was tested by comparing the adsorption capacity for different successive adsorption/desorption cycles. The adsorption capacities for five cycles were found to be 152.86 - 143.87 - 138.93 - 137.78 - 134.41 mg/g from the 1<sup>st</sup> to the 5<sup>th</sup> cycle, respectively. It is clear that, the adsorption capacity progressively decreases by increasing the cycle number. The relative adsorption capacities which were calculated with reference to the adsorption capacity at the first cycle were found to be 94.12% - 90.89% - 90.13% - 87.93% from the 2<sup>nd</sup> to the 5<sup>th</sup> cycle, respectively. The comparison of the relative adsorption capacities shows that, at the end of the fifth cycle the adsorption decreases by 12.07 %. However, until the end of the fourth cycle, the adsorption capacity was decreased only by less than 10 % which means that the acidified urea solution desorption allows effective recycling of the sorbents.

#### *Uranium leaching from Sela ore material*

A technological representative sample of Sela uranium ore material from southern eastern desert of Egypt with uranium assay of 1034 ppm was collected from granitic rocks of G. El-Sella shear zone. The uranium mineralization was mainly of the oxidized type, where it was consists essentially of secondary uranium minerals such as uranophane, beta-uranophane. Also, *B*-Autonite was observed in the shear zone besides uranophane and beta-uranophane. Secondary uranium minerals occur either disseminated or as cavity filling. Besides the presence of some accessory minerals, monazite, fluorite and apatite which are considered as the main sources for rare earth elements [45].

Commonly, the selection of a particular leaching procedure for dissolving uranium mineral is usually considered to depend essentially on the physical characteristics of the ore such as type of mineralization, ease of liberation and the nature of other constituent minerals presents [46]. Herein,

uranium is already present under its oxidized form which is interesting for acidic leaching since the addition of oxidizing agent is not necessary for improving metal recovery. Also, acidic leaching was used as it has the advantages of being more effective and requiring lower temperatures and leaching times. Moreover, the particle size from the grinding process needs only relative coarse grinding and does not need to be very small, as it is required in case of alkaline leaching. Also, sulfuric acid was used as leaching agent, which typically combines high leach performance with comparatively mild acid concentration and relatively low cost [47], in addition to be convenient for subsequent recovery process. However, sulfuric acid leaching may be has a principle disadvantage that, the acid could dissolve undesired impurities from the ore.

#### *Effect of acid concentration*

The effect of sulfuric acid concentration on uranium leaching efficiency was investigated in the range from 20 to 100 g/l, while other variables were fixed at 10 gm of ore sample with grain size below 100 mesh (inferior to 150  $\mu\text{m}$ ) and liquid/solid weight ratio 2 with agitation time of 60 minutes at 350 rpm and room temperature. The obtained results are shown in Figure 5a. From the obtained results, we could observe that there is a gradual improvement in uranium leaching efficiency was associated with increasing of acid concentration. From Figure 5a, uranium leaching efficiency exhibits a regular increasing with a relatively faster rate till sulfuric acid concentration of 80 g/l with leaching efficiency of 84.65 %. While with acid concentration of 100 g/l a slight increase was detected, this may be due to the increasing of hydrogen ion concentration in the solution that may be lead to the dissolution of some gangue materials. Moreover, the mild acid concentration of 60 g/l was found to be enough to achieve uranium leaching efficiency of 68.49 %. Hence, it was considered for further optimization of the leaching conditions in order to determine the impact of the other variables under study.

#### *Effect of leaching time*

The effect of leaching time on uranium leaching efficiency was investigated in the range from 30 to 180 minutes, while other variables were fixed at 10 gm of ore sample with grain size below 100 mesh

and liquid/solid weight ratio 2 with sulfuric acid concentration of 60 g/l and agitation at 350 rpm and room temperature. The obtained results are shown in Figure 5b. From the experimental results, it is clear that uranium leaching efficiency was gradually increased by increasing leaching time from 30 and till 150 minutes with irregular rate. The leaching efficiency was reached 90 % at leaching time of 150 minutes, while extended leaching time above 150 minutes has a minor effect on the leaching efficiency. However, leaching time of 90 minutes was found to be sufficient to achieve uranium leaching efficiency of 74.86 % which was used in further optimization of the leaching conditions in order to observe the effect of the other variables.

#### *Effect of liquid/solid weight ratio*

The effect of liquid/solid weight ratio (pulp density) on uranium leaching efficiency was investigated in the range from 1 to 4, while other variables were fixed at 10 gm of ore sample with grain size below 100 mesh and sulfuric acid concentration of 60 g/l with agitation time of 90 minutes at 350 rpm and room temperature. The obtained results are shown in Figure 5c. It is clearly obvious that, the increase in uranium leaching efficiency was closely associated with increasing of the liquid/solid ratio. This may be attributed to the decrease of solution bulk density which increases the chance of liberated uranium ions for migration to the liquid phase. Also, it may be due to the increased contact that makes the ore surface areas easily to be attacked by the acid with the more homogeneous solution. Therefore, increasing of liquid/solid ratio has a positive effect on the uranium leaching efficiency. It is worthy to mention that, uranium leaching efficiency close to 92 % could be reached using liquid/solid ratio 4. However, liquid/solid ratio of 3 with uranium leaching efficiency of 86.27 % was used in further optimization of the leaching conditions in order to observe the effect of leaching temperature.

#### *Effect of leaching temperature*

The effect of leaching temperature on uranium leaching efficiency was investigated in the range from 25 to 85  $^{\circ}\text{C}$ , while other variables were fixed at 10 gm of ore sample with grain size below 100 mesh, liquid/solid weight ratio 3, sulfuric acid concentration

of 60 g/l and agitation time of 90 minutes at 350 rpm. The obtained results are shown in Figure 5d. The obtained data revealed that, increasing the temperature from 25 up to 85 °C improved uranium leaching efficiency from 86.27 to about 94.5 % at leaching temperature of 85 °C. However, it could be

safely concluded that the temperature of 45°C with leaching efficiency of 92 % is the most suitable for practical application where after which the rate of uranium leaching efficiency increasing becomes slower.

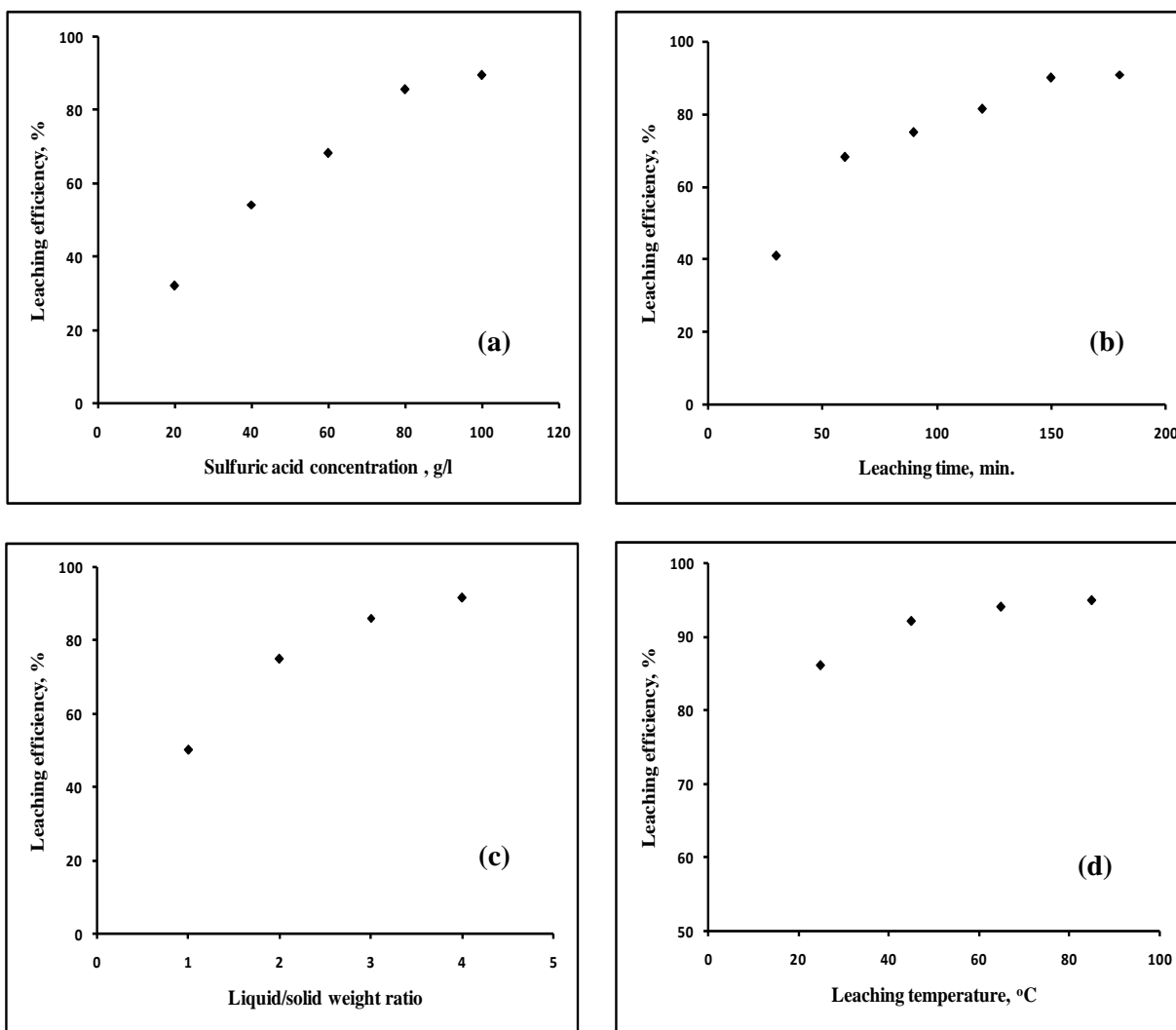


Fig. 5. Effect of different variables on uranium leaching efficiency.

#### Uranium recovery from Sela ore material

##### Preparation of leach liquor

Depending on the foregoing results of leaching conditions optimization, it can be concluded that the most suitable leaching conditions can be considered with respect to economic aspects for dissolving about 92 % of the uranium content from the ore sample would be summarized as the following: sulfuric acid concentration of 60 g/l, agitation leaching time of 90

minutes at leaching temperature of 45°C and the liquid/solid weight ratio 3 was used instead of 4 to reduce the dilution of the obtained leach liquor. Therefore, the optimized agitation acid leaching experiment was performed on 350 gram of ore sample with grain size below 100 mesh and assay of 1034 ppm (with uranium content of 361.90 mg present in the sample), under previous mentioned leaching conditions in order to prepare the stock

leach liquor. The obtained filtrate and washes were adjusted to a certain volume representing the leach liquor which was analyzed for its uranium content. While, the ore residue left behind was thoroughly washed by distilled water, then dried at 110 °C, weighed, ground and attacked by acid mixture, then was subjected to complete chemical analysis. The obtained data are given in Table 1.

The concentration of leach liquor obtained was found to be 237.32 mg/l and its volume was reached 1400 ml (leaching solution and washes) from which we could observe that the leached amount of uranium was 332.25 mg and therefore nearly about 92% of uranium content could be leached from the ore sample. The pH of the obtained leach liquor was found to be 1.97 which is much lower than that required for uranyl ions adsorption, and the increasing of the pH value would cause the precipitation of iron which usually accompanied with partially loss of uranium. Therefore, the iron was firstly precipitated at pH 3.5-4 by selective neutralization of solutions with 10 % NaOH [46]. Fortunately, different iron precipitates as an oxide, oxy-hydroxide and/or a hydroxy salt, may be contribute in the removal of impurities can be present in the leach liquor.

From the results shown in Table 1, we could observe that, about 2.76% from iron oxide of the ore percentage and which represents about 45% of total iron content in the sample was leached within the obtained leach liquor. It is well known now that, iron is considered among the common interfering elements for uranium adsorption which forms anionic sulfate species in the form of  $\text{Fe}(\text{SO}_4)_2^{-1}$ , and amine functionality present in adsorbent phase was readily extracting any anionic species from aqueous solution. Hence, the adsorbent will suffer from impaired performance in the presence of iron, which could cause the suppression of uranium uptake [2, 3]. Therefore, the removal of iron from leach liquor has positive effects specifically in terms of solution purification and improvement of uranium adsorption. After iron cake precipitation, the treated leach liquor was analyzed for its uranium content in order to determine the amount of uranium would be adsorbed within the iron hydroxides and it was found to be 51 mg. While, the residual uranium content was found to be 281.25 mg/1400 ml with uranium concentration of

200.89 mg/l and the liquor now should be contains the minimum value of total iron content.

#### *Uranium adsorption and desorption*

In general, solutions contain high concentrations of uranium would be require a preliminary extraction step by selective precipitation and/or solvent extraction as commonly followed. While the solid/liquid adsorption systems were especially optimized for processing of diluted and/or very diluted solutions with large volumes in order to separate and concentrate the target metal ions in much lower volume, which reflect the principal advantage of these systems for reducing the volume of uranium bearing solutions. Here, the prepared magnetic-polyamine chitosan adsorbent as a representative of these adsorption systems was tested in order to evaluate its applicable adsorption ability, as well as, the sensitivity of the adsorption process and its performance to real leach liquor under the same conditions of uranium mining industry with the presence of interfering elements.

**TABLE 1. Chemical analysis of Sela ore material.**

Oxide	Wt. Percent, %	
	Sample	Residue
SiO <sub>2</sub>	65.91	62.21
Al <sub>2</sub> O <sub>3</sub>	14.63	12.14
Fe <sub>2</sub> O <sub>3</sub>	6.13	3.37
CaO	1.36	2.98
MgO	0.69	1.93
MnO	0.05	0.04
Na <sub>2</sub> O	0.68	0.89
K <sub>2</sub> O	1.93	2.18
TiO <sub>2</sub>	1.45	1.83
P <sub>2</sub> O <sub>5</sub>	0.61	0.52
L.O.I	6.15	11.34
U	0.1	-
<b>Total</b>	<b>99.69</b>	<b>99.43</b>

Batch adsorption experiment was carried out under the optimized conditions of pH 4 and adsorption time 60 minutes at 250 rpm and room temperature. Initial uranium concentration of 200 mg/l was chosen depending on the previous obtained

results from which we could observe that the adsorption capacity was only increased from 152.86 mg/g to 158.43 mg/g by increasing initial uranium concentration from 200 mg/l to 300 mg/l. This means that, by increasing initial concentration by 50% adsorption capacity was only increased by 3.64%, which makes the using of initial concentration of 300 mg/l not valuable and worthless. Therefore, requisite volume from the obtained sulfate leach liquor equal to one liter with uranium concentration of 200.89 mg/l and uranium content of 200.89 mg was only used. The applied weight of magnetic-polyamine chitosan adsorbent should be in agreement with the previous studied adsorbent dosage (100 mg/100 ml); therefore one gram of adsorbent was placed in

contact with one liter leach liquor in appropriate glassware and then was stirred at room temperature until equilibrium was reached. After equilibrium and phase separation, the residual uranium concentration in the aqueous was determined and consequently the concentration of uranium ions adsorbed on the adsorbent phase was obtained by mass balance equation. The adsorption capacity was found to be 132.98 mg/g which represents only about 87% from the adsorption capacity for synthetic solution at the same conditions. The observed decrease in the uptake (by 13 %) may be due to the presence of various foreign metal ions in the feed solution such as rare earth elements and remaining iron and other traces species which could be co-adsorbed with uranium.

**TABLE 2. The results of ore leaching, uranium adsorption and desorption processes.**

<b>Ore leaching</b>	<b>Efficiency</b>	<b>Uranium content</b>
Uranium ore assay	100%	1034 ppm (g/ton)
Uranium content in 350 g sample	100%	361.90 mg
Uranium leached	92 %	332.25 mg
Leach liquor treatment (iron-free)	84.65 %	281.25 mg
<b>Uranium adsorption</b>	<b>Efficiency</b>	<b>Uranium content</b>
Adsorption capacity per gram	100%	152.86 mg
Adsorbed uranium content	87%	132.98 mg
Desorbed uranium content	84.22%	112 mg
<b>Overall recovery</b>	<b>Efficiency</b>	<b>Uranium content</b>
Uranium content in feed solution	100%	200.89 mg
Adsorbed uranium content	66.19%	132.98 mg
Recovered uranium content	55.75%	112 mg

Uranium desorption was performed according to the previously considered procedure by using portions of 30 ml urea solution 0.5 mol/l acidified with a few drops of sulfuric acid 0.2 mol/l and contact time of 30 minutes at room temperature. In order to reduce the eluted uranium solution to the lowest volume, a stepwise desorption was utilized and after each step the obtained fraction was analyzed for its uranium concentration till it was nil which reflect achieving desorption equilibrium. All fractions of the eluted uranium solution was collected and its uranium content was determined and it was

used for further calculation of the desorption efficiency. It has been found that, uranium desorption efficiency attain 84.29%. The obtained results for ore leaching, uranium adsorption and desorption were summarized in Table 2. From which we could conclude that, from 200.89 mg uranium content present in the feed solution and available for adsorption only 132.98 mg was adsorbed with uranium recovery efficiency of 66.19 %, however, the adsorbed amount represents 87% from the adsorption ability of the adsorbent from pure synthetic solution, also from the adsorbed amount of

uranium only 112 mg was desorbed with desorption efficiency of 84.22%. Finally, in spite of the complex composition of the feed solution with the presence of competitor metals which have a potential impact on uranium adsorption performance, however, the adsorbent was relatively maintained high adsorption affinity for uranium with adsorption capacity of

132.98 mg/g which considered being comparable to that obtained with the most commonly applied ion exchange resins and in sometimes better than some of them, Table 3 gives an overview on the adsorption ability of some commercial ion exchange resins for uranium which reflects the potentiality of the present adsorbent against other materials.

**TABLE 3. Uranium adsorption capacities of some commercial ion exchange resins.**

Resin type	Adsorption capacity	Reference
Dowex M4195	78 mg/g	[3]
Amberlite IR120	106.1 mg/g	[48]
Amberlite IRA -910	64.26 mg/g	[49]
Amberlite CG-400	112.36 mg/g	[50]
Doulite A101	161.84 mg/g	[51]
Ambersep 920 U (SO <sub>4</sub> )	58 mg/g	[52]
Ambersep 920 U (Cl)	50 mg/g	[53]
Amberlite IR-118H	138 mg/g	[54]
Amberlite IRA 67	56.64 mg/g	[55]
Lewatit MP 62	67.35 mg/g	[55]
Lewatit Mono Plus M500	112 mg/g	[56]
Amberjet 1200 H	130 mg/g	[57]
Modified chitosan	132.98 mg/g	This work

## Conclusions

Magnetic chitosan adsorbent has been developed, cross-linked and modified with triethylenetetramine grafting. Amino group content in the modified adsorbent was found to be 4.28 mmol/g, which means that, it is becomes about two times greater than that before grafting. Uranyl ions have been adsorbed efficiently with maximum adsorption capacity of 158.43 mg/g from synthetic sulfuric media at pH 4 and shaking time of 60 minutes with initial uranium concentration of 300 mg/l. Uranyl ions appear to be adsorbed by combined chelation and anion-exchange mechanisms. The adsorbent was efficiently regenerated using urea solution of 0.5 mol/l acidified with a few drops of sulfuric acid 0.2 mol/l and it was recycled for at least five successive cycles of adsorption/desorption with limited decrease in the performance. Uranium ore sample was subjected to acid conventional leaching through direct agitation with sulfuric acid and the relevant variables affecting leaching efficiency such as acid concentration, liquid/solid weight ratio, leaching time

and temperature were optimized and the leaching efficiency was attains 92%. The adsorption capacity from sulfuric leach liquor of Sela ore sample was found to be 132.98 mg/g with adsorption efficiency of 87%, from the adsorption ability for synthetic solutions at the same conditions and the desorption efficiency was found to be 84.22%. Finally, in spite of the complex composition of the feed solution with the presence of competitor metals which have a potential impact on uranium adsorption performance, the adsorbent was relatively maintained high adsorption affinity for uranium with adsorption capacity can be considered as comparable to that obtained with the commonly applied ion exchange resins and in sometimes better than some of them.

## References

1. Edwards C.R., and Oliver A.J, Uranium processing: A review of current methods and technology. *JOM*, 52, 12–20 (2000).
2. Moon E.M., Ogden M.D., Griffith C.S., Wilson A., and Mata J.P., Impact of chloride on uranium(VI)

- speciation in acidic sulfate ion exchange systems: Towards seawater-tolerant mineral processing circuits. *J. Ind. Eng. Chem.*, 51, 255–263 (2017).
- Ogden M.D., Moon E.M., Wilson A., and Pepper S.E., Application of chelating weak base resin Dowex M4195 to the recovery of uranium from mixed sulfate/chloride media. *Chem. Eng. J.*, 317, 80–89 (2017).
  - Habib M., Hafida M., Abdelkader T., Caroline B. and Anne B., Study on the extraction of lanthanides by a mesoporous MCM-41 silica impregnated with Cyanex 272. *Sep. Purif. Technol.*, 209, 359–367 (2019)
  - Wang Q., Chang X., Hu Z., Li D., Li R. and Chai X., Preconcentration of erbium(III) ions from environmental samples using activated carbon modified with benzoyl hydrazine. *Microchim. Acta*, 172 395–402 (2011).
  - Mahfouz M.G., Killa H.M., Sheta M.E., Moustafa A.H. and Tolba A.A., Synthesis, characterization, and application of polystyrene adsorbents containing tri-n-butylphosphate for solid-phase extraction of uranium (VI) from aqueous nitrate solutions. *J. Radioanal. Nucl. Chem.*, 301, 739–749 (2014).
  - Dong Z., Liu J., Yuan W., Yi Y. and Zhao L., Recovery of Au(III) by radiation synthesized aminomethyl pyridine functionalized adsorbents based on cellulose. *Chem. Eng. J.*, 283, 504–513 (2016).
  - Wang J., He B., Wei X., Li P., Liang J., Qiang S., Fan Q. and Wu W., Adsorption of uranyl ions on TiO<sub>2</sub>: effects of pH, contact time, ionic strength, temperature and HA. *J. Environ. Sci.*, 75, 115–123 (2019).
  - Wazne M., Meng X., Korfiatis G.P. and Christodoulatos C., Carbonate effects on hexavalent uranium removal from water by nanocrystalline titanium dioxide. *J. Hazard. Mater.*, 136, 47–52 (2006).
  - Liu P., Wu H., Yuan N., Liu Y., Pan D. and Wu W., Removal of U(VI) from aqueous solution using synthesized beta-zeolite and its ethylene-diamine derivative. *J. Mol. Liq.*, 234, 40–48 (2017).
  - Shakur H.R., Saraee K.R.E., Abdi M.R. and Azimi G., Selective removal of uranium ions from contaminated waters using, modified-X nanozeolite. *Appl. Radiat. Isot.*, 118, 43–55 (2016).
  - Khayambashi A., Wang X. and Wei Y., Solid phase extraction of uranium (VI) from phosphoric acid medium using macroporous silica-based D2EHFA-TOPO impregnated polymeric adsorbent. *Hydrometallurgy* 164, 90–96 (2016).
  - Gdula K., Gładysz-Płaska A., Cristóvão B., Ferenc W. and Skwarek E., Amine-functionalized magnetite-silica nanoparticles as effective adsorbent for removal of uranium(VI) ions. *J. Mol. Liq.*, 290, 111217 (2019).
  - Joseph C., Schmeide K., Sachs S., Brendler V., Geipel G. and Bernhard G., Adsorption of uranium(VI) onto Opalinus Clay in the absence and presence of humic acid in Opalinus Clay pore water. *Chem. Geol.*, 284, 240-250 (2011).
  - Gładysz-Płaska A., Grabias E. and Majdan M., Simultaneous adsorption of uranium(VI) and phosphate on red clay. *Prog. Nucl. Energ.*, 104, 150-159 (2018).
  - Mellah A., Chegrouche S. and Barkat M., The removal of uranium(VI) from aqueous solutions onto activated carbon: Kinetic and thermodynamic investigation. *J. Colloid Interface Sci.*, 296(2), 434-441 (2006).
  - Morsy A.M.A. and Hussein A.E.M., Adsorption of uranium from crude phosphoric acid using activated carbon. *J. Radioanal. Nucl. Chem.*, 288, 341–346 (2011).
  - Fan F.L., Qin Z., Bai J., Rong W.D., Fan F.Y., Tian W. and Zhao L., Rapid removal of uranium from aqueous solutions using magnetic Fe<sub>3</sub>O<sub>4</sub>@SiO<sub>2</sub> composite particles. *J. Environ. Radioact.*, 106, 40–46 (2012).
  - Alqadami A.A., Naushad M., Alothman Z.A. and Ghfar A.A., Novel metal-organic framework (MOF) based composite material for the sequestration of U(VI) and Th(IV) metal ions from aqueous environment. *ACS Appl. Mater. Interfaces*, 9, 36026–36037 (2017)
  - Erkaya I.A., Arica M.Y., Akbulut A. and Bayramoglu G., Bioadsorption of uranium(VI) by free and entrapped *Chlamydomonas reinhardtii*: kinetic, equilibrium and thermodynamic studies. *J. Radioanal. Nucl. Chem.*, 299, 1993–2003 (2014).
  - Galhoum A.A., Mahfouz M.G., Atia A.A., Abdel-Rehem S.T., Gomaa N.A., Vincent T. and Guibal E., Amino acid functionalized chitosan magnetic nano-based particles for uranyl sorption. *Ind. Eng. Chem. Res.*, 54, 12374-12385 (2015).
  - El-Bohy M.N., Abdel-Monem Y.K., Rabie K.A., Farag N.M., Mahfouz M.G., Galhoum A.A. and Guibal E., Grafting of arginine and glutamic acid onto cellulose for enhanced uranyl sorption. *Cellulose*, 24, 1427-1443 (2017).
  - Elsalamouny A.R., Desouky O.A., Mohamed S.A., Galhoum A.A. and Guibal E., Uranium and

- Neodymium bioadsorption using novel chelating polysaccharide. *Int. J. Biol. Macromol.*, 104, 963-968 (2017).
24. Konishi Y., Shimaoka J.I., Asai S., Adsorption of rare-earth ions on biopolymer gel beads of alginic acid. *React. Funct. Polym.*, 36, 197-206 (1998).
  25. Goel N.K., Kumar V., Misra N. and Varshney L., Cellulose based cationic adsorbent fabricated via radiation grafting process for treatment of dyes waste water. *Carbohydr. Polym.*, 132, 444-451 (2015).
  26. Kolodynska D., Chitosan as an effective low-cost adsorbent of heavy metal complexes with the polyaspartic acid, *Chem. Eng. J.*, 173, 520- 529 (2011).
  27. Hiroki A., Tran H.T., Nagasawa N., Yagi T. and Tamada M., Metal adsorption of carboxymethyl cellulose/carboxymethyl chitosan blend hydrogels prepared by Gamma irradiation. *Radiat. Phys. Chem.*, 78, 1076-1080 (2009).
  28. Babel S. and Kurniawan T.A., Low-cost adsorbents for heavy metals uptake from contaminated water: a review, *J. Hazard. Mater.*, 97, 219-243 (2003).
  29. Boamah P.O., Huang Y., Hua M., Zhang Q., Wu J., Onumah J., Sam-Amoah L.K., Boamah P.O., Adsorption of heavy metal ions onto carboxylate chitosan derivatives-A mini-review, *Ecotoxicol. Environ. Saf.*, 116, 113-120 (2015).
  30. Kousalya G.N., Gandhi M.R. and Meenakshi S., Adsorption of chromium(VI) using modified forms of chitosan beads. *Int. J. Biol. Macromol.*, 47, 308-315 (2010).
  31. Gandhi M.R., Kousalya G.N., Viswanathan N. and Meenakshi S., Adsorption behaviour of copper on chemically modified chitosan beads from aqueous solution. *Carbohydr. Polym.*, 83, 1082-1087 (2011).
  32. Marczenko Z., Spectrophotometric determination of elements, Ellis Horwood, Chichester (U.K.), 1976.
  33. Namdeo M. and Bajpai S.K., Chitosan-magnetite nanocomposites (CMNs) as magnetic carrier particles for removal of Fe(III) from aqueous solutions. *Colloids Surf., A*, 320, 161-168 (2008).
  34. Ngah W.S.W., Endud C.S. and Mayanar R., Removal of copper(II) ions from aqueous solution onto chitosan and cross-linked chitosan beads, *React. Funct. Polym.*, 50(2), 181-190 (2002).
  35. Oshita K., Takayanagi T., Oshima M. and Motomizu S., Adsorption behavior of cationic and anionic species on chitosan resins possessing amino acid moieties, *Anal. Sci.*, 23, 1431-1434 (2007).
  36. Elwakeel K.Z., Atia A.A. and Donia A.M., Removal of Mo(VI) as oxoanions from aqueous solutions using chemically modified magnetic chitosan resins. *Hydrometallurgy*, 97, 21-28 (2009).
  37. Davies W. and Gray W., A Rapid and specific method for the precise determination of uranium using iron (II) sulfate as reductant. *Talanta*, 11, 1203-1211 (1964).
  38. Xue X., Wang J., Mei L., Wang Z., Qi K. and Yang B., Recognition and enrichment specificity of Fe<sub>2</sub>O<sub>3</sub> magnetic nanoparticles surface modified by chitosan and *Staphylococcus aureus* enterotoxins A antiserum. *J. Colloids Surf., B*, 103, 107-113 (2013).
  39. Li G.Y., Jiang Y.R., Huang K.L., Ding P. and Chen J., Preparation and properties of magnetic Fe<sub>3</sub>O<sub>4</sub>-chitosan nanoparticles. *J. Alloys Compd.*, 466(1-2), 451-456 (2008).
  40. Grenthe I., Drozdowski J., Fujino T., Buck E.C., Albrecht-Schmitt T. E. and Wolf S.F., Uranium: The Chemistry of the Actinide and Transactinide Elements, 3 ed., Vol. 1; Morss L. R., Edelstein N. M., Fuger J., Eds. Springer: Dordrecht, The Netherlands (2006).
  41. Simsek S., Yilmaz E. and Boztug A., Amine-modified maleic anhydride containing terpolymers for the adsorption of uranyl ion in aqueous solutions. *J. Radioanal. Nucl. Chem.*, 298(2), 923-930 (2013).
  42. Gao Y.H., Oshita K., Lee K.H., Oshima M. and Motomizu S., Development of column-pretreatment chelating resins for matrix elimination/multi-element determination by inductively coupled plasma-mass spectrometry. *Analyst* 127, 1713-1719 (2002).
  43. Donia A.M., Atia A.A., El-Boraey H.A. and Mabrouk D.H., Adsorption of Ag(I) on glycidyl methacrylate/N, N'-methylene bis-acrylamide chelating resins with embedded iron oxide. *Sep. Purif. Technol.*, 48(3), 281-287 (2006).
  44. Ritcey G.M. and Ashbrook A.W., Solvent Extraction: Principles and Applications to Process Metallurgy. Part I, Elsevier Publishers, Amsterdam (1984).
  45. Ibrahim T.M., Ali K.G., Gaafar I.M., Masoud S.M., Omer S.A., Shahin H.A., Haridy M.M., Aly E.M., Biomy M., Abdel-Gawad A., Abo-Donia A., Abdel-Monsef M. and Awad M., Extensive studies on G. El-Sella Shear zone South Eastern Desert, Egypt. *Int. report, N.M.A., Cairo, Egypt*, 91 (2005).
  46. Merritt R.C., The Extractive Metallurgy of Uranium, Colorado School of Mines Res. Inst., Golden,

- Colorado (1971).
47. Bhargava S.K., Ram R., Pownceby M., Grocott S., Ring B., Tardo J. and Jones L., A review of acid leaching of uraninite. *Hydrometallurgy*, 151, 10-24 (2015).
48. Gawad E.A., Uranium removal from nitrate solution by cation Exchange resin (Amberlite IR 120), adsorption and kinetic Characteristics. *Nuclear Sciences Scientific Journal*, 8, 213-230 (2019).
49. Rahmati A., Ghaemi A. and Samadfam M., Kinetic and thermodynamic studies of uranium (VI) adsorption using Amberlite IRA-910 resin. *Ann. Nucl. Energy*, 39, 42-48 (2012).
50. Semnani F., Asadi Z., Samadfam M. and Sepehrian H., Uranium(VI) adsorption behavior onto Amberlite CG-400 anion exchange resin: effects of pH, contact time, temperature and presence of phosphate. *Ann. Nucl. Energy*, 48, 21-24 (2012).
51. Khalifa M.E., Selective separation of uranium using alizarin red S (ARS)-modified anion-exchange resin or by flotation of U-ARS chelate. *Sep. Sci. Technol.*, 33, 2123-2141(1998).
52. Cheira M.F., Atia B.M. and Kouraim M.N., Uranium(VI) recovery from acidic leach liquor by Ambersep 920U SO<sub>4</sub> resin: Kinetic, equilibrium and thermodynamic studies. *J. Radiat. Res. Appl. Sc.*, 10(4), 307-319 (2017).
53. Cheira M.F., El-Didamony A.M., Mahmoud K.F. and Atia B.M., Equilibrium and Kinetic Characteristics of Uranium Recovery by the Strong Base Ambersep 920U Cl Resin, *IOSR-JAC*, 7(5), 32-40 (2014).
54. Kilislioglu A. and Bilgin B., Thermodynamic and kinetic investigations of uranium adsorption on amberlite IR-118H resin. *Appl. Radiat. Isot.*, 58,155-160 (2003).
55. Riegel M., Tokmachev M. and Hoell W.H., Kinetics of uranium adsorption onto weakly basic anion exchangers, *React. Funct. Polym.*, 68, 1072-1080 (2008).
56. Khawassek Y.M., Anion exchange of uranium from sulfuric acid solution: adsorption and kinetics characteristics, In proceedings of ALTA uranium-REE conference including lithium processing forum, ALTA Metallurgical Services, Perth, Australia, 126-140 (2017).
57. Khawassek Y.M., Masoud A.M., Taha M.H. and Hussein A.E.M., Kinetics and thermodynamics of uranium ion adsorption from waste solution using Amberjet 1200 H as cation exchanger, *J. Radioanal. Nucl. Chem.*, 315, 493-502 (2018).